🔓 **Open Access**

Effects of Aerosol Mixing States on the Aerosol Multiple Scattering Properties and the Light Transmittances

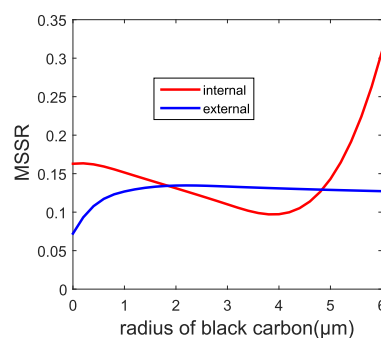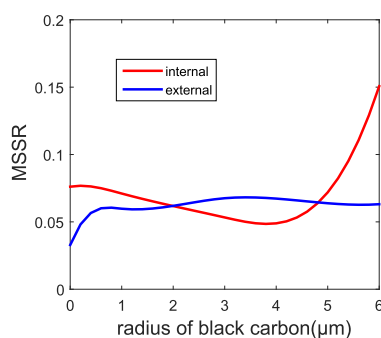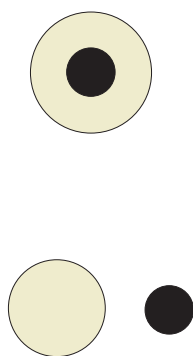**Yuzhao Ma**
Wenrong Liu
Huiliang Gao
Jiaqi Liu
Meng Li
Xinglong Xiong

Effects of Aerosol Mixing States on the Aerosol Multiple Scattering Properties and the Light Transmittances

Yuzhao Ma [ID],[1,2] **Wenrong Liu,**[2] **Huiliang Gao,**[2] **Jiaqi Liu,**[2]
Meng Li [ID],[3] **and Xinglong Xiong**[1,2]

[1]Tianjin Key Laboratory for Advanced Signal Processing, Civil Aviation University of China,
Tianjin 300300, China
[2]College of Electronic Information and Automation, Civil Aviation University of China, Tianjin
300300, China
[3]Institute of Civil Aviation Meteorological Technology, Civil Aviation University of China,
Tianjin 300300, China

Abstract: The scattering properties of atmospheric aerosols may be sensitive to the mixing states of the aerosols. Based on the internal and external mixing models of the aerosols, we have numerically simulated the transmissions of the light through mixed aerosols using the Monte-Carlo method. For the first time, the multiple scattering properties of mixed aerosols are discussed for different mixing states of the aerosol systems composing of black carbon and sulfate, considering different sizes of the black carbon particle. The simulation results show that the mixing states may significantly affect the multiple scattering properties of aerosols, hence, the light transmittances. The presented work is useful for better understanding the light transmission through the actual aerosols.

Index Terms: Multiple scatterings, mixing state, Monte-Carlo method.

1. Introduction

With the development of laser technology and the need for the wireless optical communication, the propagation of the light through the atmosphere is receiving more and more attentions [1]–[3]. It is known that the actual atmosphere composes of different aerosol components with different mixing states. A number of scientists have focused their research on the mixing states of atmospheric aerosols. Riemer has studied the aging process of black carbon aerosols. He presented that the black carbon aerosols were hydrophobic when they were released newly into the atmosphere, and would mix with other aerosols in different forms with time [4]. Ma has studied the daily changes of black carbon aerosols. It was shown that the black carbon aerosols tended to mix externally with other aerosols during the day, while tended to mix internally with other aerosols at the night [5].

The aerosol mixing states may affect the scatterings of the light through the aerosols [6]–[8]. Based on the Mie scattering theory, Zhou has calculated the scattering, absorption and extinction coefficients of aerosols of different mixing states. It was pointed out that the mixing state and mixing ratio of aerosols had significant influences on the scattering properties of the light through aerosols

[9]. Moreover, multiple scattering effects of light through aerosols have attracted interests recently. The multiple-scattering effects of the light are of interest for that the multiple scattering components are indiscriminately captured by the optoelectronic detector of the measurement systems, while only first-order scattering component is considered in the classic scattering theory. The multiple-scattering effects are significant, especially for large fields of view in the low visibility atmosphere due to large density of the aerosols [10]. Elkamchouchi has discussed the multiple scatterings of the light pulse through cloud of different optical thicknesses [11]. Wang has studied the attenuation of laser light considering the multiple scattering effects in different types of aerosols [12]. Otsuki has investigated the effects of multiple scatterings on the optical rotation and the polarization characteristics in turbid media [13]. Nevertheless, up to now, the effects of aerosol mixing states on the aerosol multiple scattering properties have not been investigated.

We have noted the light transmission through atmospheric aerosols of different mixing states has been discussed in several applications. Cheng has studied the effects of the aerosol mixing state on the upward radiance/polarization and hemispheric flux of soot aerosols using the vector radiative transfer model [14]. Wang has studied the effects of the mixing state of black carbon aerosols on reflection function and plane albedos [15]. Nevertheless, so far, the light transmission through mixed aerosols, considering multiple-scattering effects, has not been reported. We perform the work in this paper.

Internal mixture and external mixture can be regarded as the principal mixing forms of aerosols in reality. Taking the aerosol systems composing of black carbon and sulfate as example, we have numerically simulated the transmission of the light through the black carbon and sulfate mixed internally and externally with each other using the Monte-Carlo method in this paper. As simulation results, the energy ratios of each scattering order and the multiple to single scattering ratio (MSSR) are presented for different sizes of black carbon particle. Furthermore, the multiple-scattering effects of the aerosols of different mixing states on the light transmittance are discussed. Our work is important for the aerosol characterizations and evaluations of the performances of a variety of systems that operate based on the light propagation through the atmosphere.

2. Mixing States of Aerosols

The atmospheric aerosols are generally multiphase systems consisting of solid and liquid particles with a particle size of $10^{-2} - 10^2$ μm suspended in the atmosphere. Typical aerosols can be black carbon, sulfate, nitrate, ammonium salt, sea salt, and even sand. In decades, quite a few Chinese cities have suffered frequent fog and haze, which are caused mainly by the burning of fossil fuels. It has been shown that black carbon and sulfate, as typical aerosols, are principal compositions of haze.

The actual atmospheric aerosols can be mixtures of different components. Aerosol components may mix with each other externally or internally. The aerosol mixing states may significantly affect the optical properties of the aerosol systems. For the external mixture, each particle corresponds to only one aerosol component, and the different aerosol particles exist independently in the atmosphere. The situation of the internal mixture is more complex. For internal mixture different aerosol components mix with each other internally in complicated forms. So far, four models have been proposed for internal mixing states of aerosols [16]: (1) Core-shell model, the non-hygroscopic components packaged by the hygroscopic components form concentric sphere structure; (2) Maxwell Garnett model, the non-hygroscopic components are randomly distributed in hygroscopic components [17]; (3) Bruggeman model, which exists in the adjacent topological relation between the different components of aerosol particles; (4) Homogeneous mixing model, the aerosols of different components are condensed into a particle, and the various components are uniformly mixed together.

Previous research shows that the black carbon, being the dominant absorber, is often co-emitted with a variety of water soluble aerosols, e.g., sulfate [4], [5]. As black carbon particles are transported in the atmosphere, external and internal mixtures of black carbon and other aerosols may be formed.
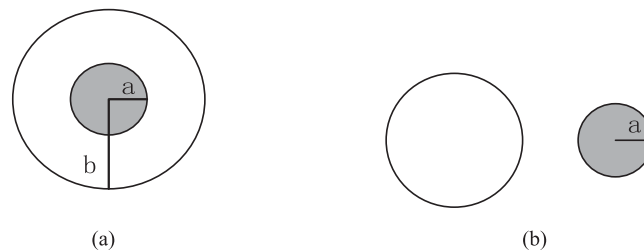
Fig. 1. Two mixing states of black carbon and sulfate. (a) Internal mixture. (b) External mixture.
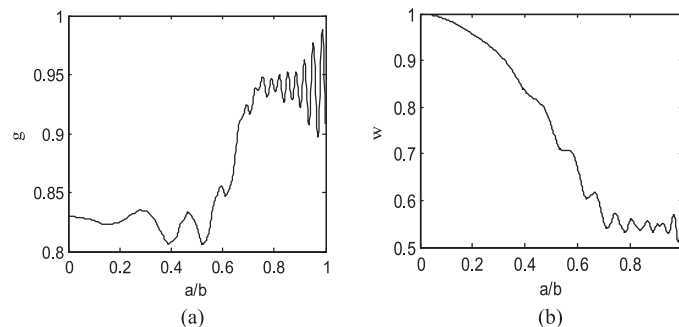

Fig. 2. Single scattering properties of the internal mixture of black carbon and sulfate with respect to a/b. (a) The asymmetry factor. (b) The single scattering albedo.

At the beginning, the black carbon usually mixes externally with water soluble aerosol. After a period of time, the black carbon, often as the core part, may mix internally with those water soluble aerosols.

In the following work, to quantitatively evaluate the effects of the aerosol mixing states on the aerosol multiple scattering properties and the light transmittances, we take the aerosol systems composing of black carbon and sulfate as example. For the internal mixture, the Core-shell model is used. We assume the black carbon particle centers inside the sulfate particle, shown in Fig. 1(a). The radius of the core component (black carbon) is assumed to be a, and the outer radius of concentric sphere is b. For the external mixture, black carbon particle is physically separated from sulfate particle, as shown in Fig. 1(b). The size of the sulfate particle for the external mixture can be calculated using a and b by assuming the constant total volume of the particles.

3. Single Scattering Properties of Mixed Aerosols

It is well known that Mie scattering theory can be used to deal with the scattering problems of homogeneous spherical particles, while its variation, the Mie scattering theory for coated spheres can be used to study the scattering problems of the concentric spherical particles. In order to investigate the effects of the aerosol mixing states on the aerosol multiple scattering properties and the light transmittances, we first use the Mie scattering theory to characterize the single scattering properties of the internal and external mixtures of black carbon and sulfate. The asymmetry factor and the single scattering albedo are the most important quantities presenting the single scattering properties of a scatter. The asymmetry factor is defined as the weighted average of the cosine of scattering angle, which represents the asymmetry of forward and backward scattering of the particles. The single scattering albedo is defined as the ratio of the scattering cross section to the extinction cross section, which represents the scattering ability of the particles.

The asymmetry factor and the single scattering albedo of the particle of internal mixture with respect to the ratio of the inner radius to the outer radius are shown in Fig. 2. In all calculations, we
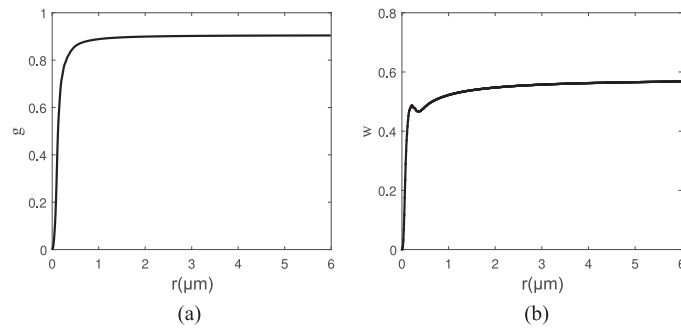
Fig. 3. Single scattering properties of the black carbon particle with respect to the particle radius. (a) The asymmetry factor. (b) The single scattering albedo.
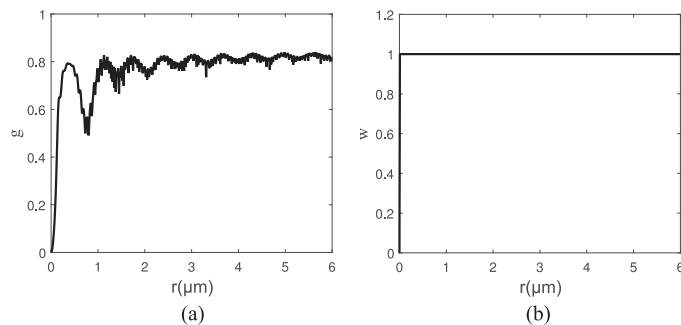

Fig. 4. Single scattering properties of the sulfate particle with respect to the particle radius. (a) The asymmetry factor. (b) The single scattering albedo.

assume the optical wavelength is 550 nm and the outer radius of concentric sphere $b = 6~\mu$m. It is seen in Fig. 2(a) that the asymmetry factor rises rapidly after the ratio a/b is 0.5 and then tends to oscillate around $g = 0.95$. The single scattering albedo decreases for $a/b < 0.6$ and then tends to oscillate around $w = 0.55$, as seen in Fig. 2(b).

On the other hand, the single scattering properties of the black carbon particle and the sulfate particle are important for studying the aerosol multiple scattering properties of the external mixture of black carbon and the sulfate. The asymmetry factor and the single scattering albedo of the black carbon particle with respect to the particle radius are shown in Fig. 3. It can be seen in Fig. 3(a) and Fig. 3(b) that the asymmetry factor and the single scattering albedo of the black carbon particle rise rapidly as the particle size for $r < 0.5~\mu$m. The asymmetry factor tends to be 0.9 and the single scattering albedo tends to be 0.56 for larger particle size. In fact black carbon is the dominant absorber in actual atmosphere.

Similarly, the asymmetry factor and the single scattering albedo of the sulfate particle with respect to the particle radius are shown in Fig. 4. It can be seen in Fig. 4(a) that the asymmetry factor of the sulfate particle oscillates around 0.80 as the scale parameter increases. It is seen in Fig. 4(b) that the single scattering albedo of the sulfate particle is almost 1 independent of the scale parameter. This indicates that the scattering effects of sulfate particle exclusively determine the extinction of the light.

We have seen from the simulation results that the black carbon and the sulfate have rather different scattering properties. The single scattering albedo of black carbon particle is smaller than that of the sulfate particle. The black carbon may absorb part of the incoming light, while the sulfate particle only scatters the light. In the following sections we will demonstrate the mixing states of the black carbon and the sulfate may affect the aerosol multiple scattering properties and the light transmittances significantly.

4. Effects of Aerosol Mixing States on the Aerosol Multiple Scattering Properties

When optical light propagates through aerosols of large density, the photons may be scattered many times. This is known as multiple scatterings. The Monte-Carlo method has seen to be efficient in evaluating the multiple scattering effects of light in a variety of media in several applications [18]–[23]. In this section, we investigate the effects of aerosol mixing states on the aerosol multiple scattering properties using the Monte-Carlo method. The single scattering properties of the black carbon particle and sulfate particle demonstrated previously are used.

4.1 Monte-Carlo Method

In the Monte-Carlo method the scattering of the light in the atmosphere is regarded as the collision of a photon with aerosol particles. The scattering angle is determined by the scattering phase function. The photon propagation distance between the successive collisions is determined by aerosol extinction coefficient. The single scattering albedo determines the variation of the light energy in the collision. The Monte-Carlo method used for investigating the effects of aerosol mixing states on the aerosol multiple scattering properties is detailed as follows.

4.1.1 Initializing a Photon: We assume that the transmitter is located at O $(0, 0, 0)$ in the Cartesian coordinate system. θ_1 is the half divergence angle of the transmitting laser beam, and the initial zenith angle θ_0 is uniformly distributed within the cone $[0, \theta_1]$. The initial azimuthal angle is assumed to be uniformly distributed within $[0, 2\pi]$. The direction cosine of the emitted photon in the Cartesian coordinates can be expressed by θ_0 and φ_0 as

$$D_0 = \begin{bmatrix} u_{x_0} \\ u_{y_0} \\ u_{z_0} \end{bmatrix} = \begin{bmatrix} \sin\theta_0 \cos\varphi_0 \\ \sin\theta_0 \sin\varphi_0 \\ \cos\theta_0 \end{bmatrix} \tag{1}$$

Additionally, the step size l is given as

$$l = -\frac{1}{\sigma} \ln r, \tag{2}$$

where σ is the atmosphere extinction coefficient, defined by the sum of extinction cross sections of all particles per unit volume, and has the unit of inverse of length. r is a random number within the range of (0,1). Consequently, the Cartesian coordinates of the first scattering center are

$$P_1(x_1, y_1, z_1) = O(0, 0, 0) + lD_0 \tag{3}$$

4.1.2 The Photon Transportation After a Collision with an Aerosol Particle: We assume the direction of the photon after a collision is denoted by θ_s and φ_s in the spherical coordinates. The azimuthal angle φ_s is uniformly distributed within $[0, 2\pi]$, similar to φ_0. The scattering of a photon is characterized by the well-known Henyey-Greenstein function as

$$P(\cos\theta_s) = \frac{1 - g^2}{4\pi(1 + g^2 - 2g\cos\theta_s)^{3/2}}, \tag{4}$$

where g stands for the asymmetry factor, defined by the average cosine of the scattering function:

$$g = \langle \cos\theta_s \rangle = \frac{1}{2} \int_{-1}^{1} P(\cos\theta_s) \cos\theta_s d(\cos\theta_s). \tag{5}$$

g usually has the range of $[-1,1]$. We may obtain the scattering angle of the new photon path by using

$$r = 2\pi \int_{-1}^{\cos\theta_s} P(\cos\theta_s) d(\cos\theta_s),$$

where r is again the random number. Upon integration we find that for $g \neq 0$

$$\theta_s = \arccos\left\{ \frac{1}{2g}\left[1 + g^2 - \left(\frac{1-g^2}{1+g-2gr} \right)^2 \right] \right\}. \qquad (6)$$

For $g = 0$,

$$\theta_s = \arccos(2r - 1).$$

The energy of the light after the mth collision of the photon is denoted by

$$E_{m+1} = w E_m, \qquad (7)$$

where w is the single scattering albedo of the particle. The initial value of E_m is 1.

After the mth collision of the photon, the direction cosine of the traveling path of the photon with respect to the original Cartesian coordinate system can be expressed as

$$\boldsymbol{D'}_m = \begin{bmatrix} \frac{\sin\theta_{s,m}}{\sqrt{1-u^2_{z_{m-1}}}}(u_{x_{m-1}}u_{z_{m-1}}\cos\varphi_{s,m} - u_{y_{m-1}}\sin\varphi_{s,m}) + u_{x_{m-1}}\cos\theta_{s,m} \\ \frac{\sin\theta_{s,m}}{\sqrt{1-u^2_{z_{m-1}}}}(u_{y_{m-1}}u_{z_{m-1}}\cos\varphi_{s,m} + u_{x_{m-1}}\sin\varphi_{s,m}) + u_{y_{m-1}}\cos\theta_{s,m} \\ -\sin\theta_{s,m}\cos\varphi_{s,m}\sqrt{1-u^2_{z_{m-1}}} + u_{z_{m-1}}\cos\theta_{s,m} \end{bmatrix}, \qquad (8)$$

where,

$$\begin{bmatrix} u_{x_{m-1}} \\ u_{y_{m-1}} \\ u_{z_{m-1}} \end{bmatrix} = \begin{bmatrix} \sin\theta_{s,m-1}\cos\varphi_{s,m-1} \\ \sin\theta_{s,m-1}\sin\varphi_{s,m-1} \\ \cos\theta_{s,m-1} \end{bmatrix}.$$

Finally we obtain the coordinates of the photon after the mth collision as

$$P_{m+1}(x_{m+1}, y_{m+1}, z_{m+1}) = P_m(x_m, y_m, z_m) + l\boldsymbol{D}_m', \qquad (9)$$

where l is produced using Equation (2). The coordinates of the photon after the mth collision are hence obtained using the coordinates of its last scattering center.

Supposing the light propagates through the internal mixture of black carbon and sulfate, the Core-shell model of the concentric sphere presented in Fig. 1(a) is used as the scatter. The asymmetry factor and the single scattering albedo presented in Fig. 2 are used in the simulations. Supposing the light propagates through the external mixture of black carbon and sulfate, the model of a black carbon particle and a sulfate particle presented in Fig. 1(b) is regarded as the scatter. The photon can be scattered either by the black carbon particle or the sulfate particle. We assume the same densities of the two types of the particles. Consequently, the photon may collide with the two types of particles with the similar probabilities. When the photon collides with a black carbon particle, the asymmetry factor and the single scattering albedo presented in Fig. 3 are used in the simulations. When the photon collides with a sulfate particle, the asymmetry factor and the single scattering albedo presented in Fig. 4 are used in the simulations.

4.1.3 Receiving a Photon: The reception of a photon is judged in terms of the detection area. In case the photon exactly reaches the detector, the photon is certainly regarded as being received by the detector. On the other hand, when the travelling path of the photon intersects with the detector area the photon may be also regarded as being received by the detector.

In the simulations, the following assumptions are done. The total number of simulated photons is normally 10^6. The distance between the transmitter and the receiver is 30 m. The emitted light has a small divergence with the half angle of divergence being $\theta_1 = 0.06$ mrad. The receiver has the full field of view and the receiver diameter is 100 cm. The outer radius of sphere of internal mixture b is 6 μm and the radius of the core (black carbon) a is assumed to be 0.1 μm, 1.0 μm, 3.0 μm, 5.0 μm, and 5.9 μm, respectively. It is assumed that the internal mixture of the concentric sphere has the same volumes with the external mixture of a black carbon particle and a sulfate particle. Consequently, the radius of the sulfate particle in the external mixture can be calculated using a and b.

TABLE 1

Single Scattering Properties of the Internal Mixture for $b = 6$ μm and different a Values

a/b	0.02	0.17	0.50	0.83	0.98
g	0.83	0.82	0.82	0.93	0.98
w	1.00	0.97	0.76	0.54	0.51

TABLE 2

Single Scattering Properties of the Black Carbon Particle of Different Sizes

Radius / μm	0.10	1.00	3.00	5.00	5.90
g	0.33	0.89	0.90	0.90	0.90
w	0.37	0.52	0.56	0.57	0.57

TABLE 3

Single Scattering Properties of the Sulfate Particle of different Sizes

Radius / μm	6.00	5.99	5.74	4.50	2.20
g	0.83	0.81	0.83	0.80	0.79
w	1.00	1.00	1.00	1.00	1.00

The asymmetry factors and the single scattering albedos of the internal mixture for $b = 6$ μm and different a values are demonstrated in Table 1. The asymmetry factors and the single scattering albedos of the black carbon particles and the sulfate particles of different sizes are demonstrated in Table 2 and Table 3, respectively. These values are used in the numerical simulations of the multiple scattering effects.

4.2 Simulation Results of the Aerosol Multiple Scattering Properties for different Aerosol Mixing States

Using the Monte-Carlo method, the multiple scattering properties of mixed aerosols are numerically simulated. The extinction coefficients of the aerosols are assumed to be from 4 to 60 km^{-1} with the step of 4 km^{-1}. The maximum scattering order is assumed to be four. The energy ratio of each scattering order and the MSSR are presented.

The energy ratios of each scattering order relative to the total received energy with respect to the extinction coefficient for the internal and external mixtures with the black carbon radius of 0.1 μm are shown in Fig. 5(a) and Fig. 5(b) in semi logarithmic scale, respectively. In order to demonstrate the multiple scattering effects clearly, the corresponding MSSRs for the internal and external mixtures are shown in Fig. 5(c). Similarly, the energy ratios of each scattering order and the MSSRs for the black carbon radius of 1.0 μm, 3.0 μm, 5.0 μm and 5.9 μm are demonstrated in Figs. 6–9, respectively. Further, the variations of MSSRs with the black carbon for both mixtures are shown
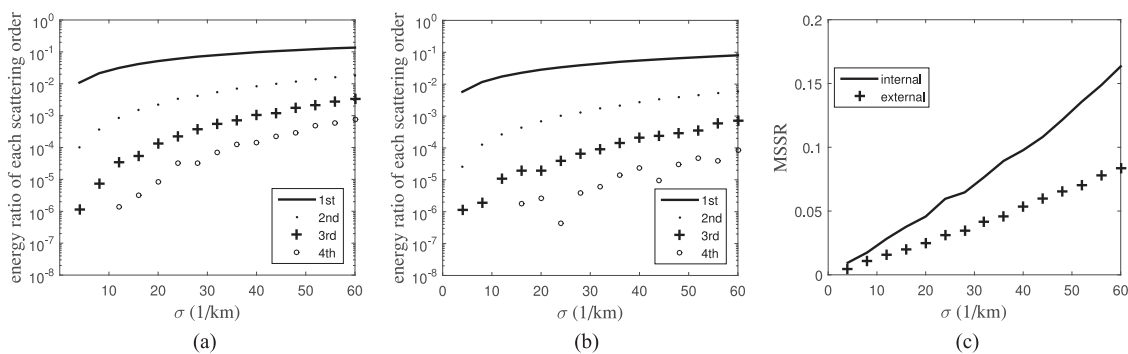
Fig. 5. Scattering properties with respect to the extinction coefficient with the black carbon radius of 0.1 μm. (a) Energy ratio of each scattering order for the internal mixture. (b) Energy ratio of each scattering order for the external mixture. (c) MSSR.

Fig. 6. Scattering properties with respect to the extinction coefficient with the black carbon radius of 1.0 μm. (a) Energy ratio of each scattering order for the internal mixture. (b) Energy ratio of each scattering order for the external mixture. (c) MSSR.
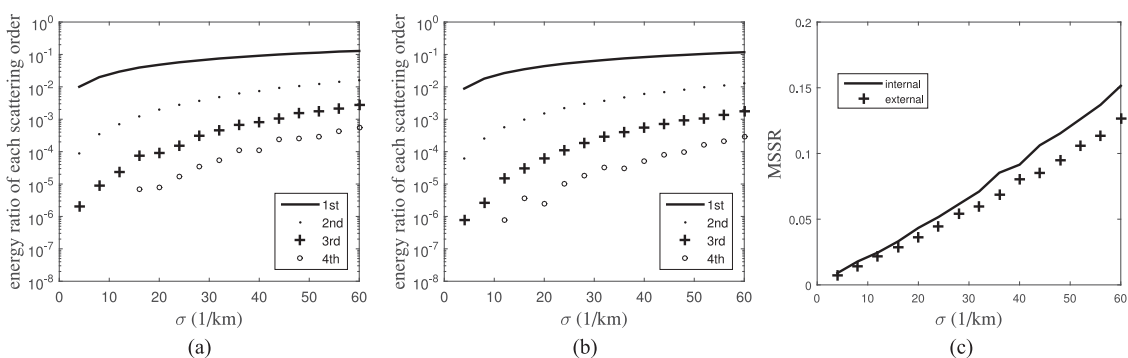

Fig. 7. Scattering properties with respect to the extinction coefficient with the black carbon radius of 3.0 μm. (a) Energy ratio of each scattering order for the internal mixture. (b) Energy ratio of each scattering order for the external mixture. (c) MSSR.
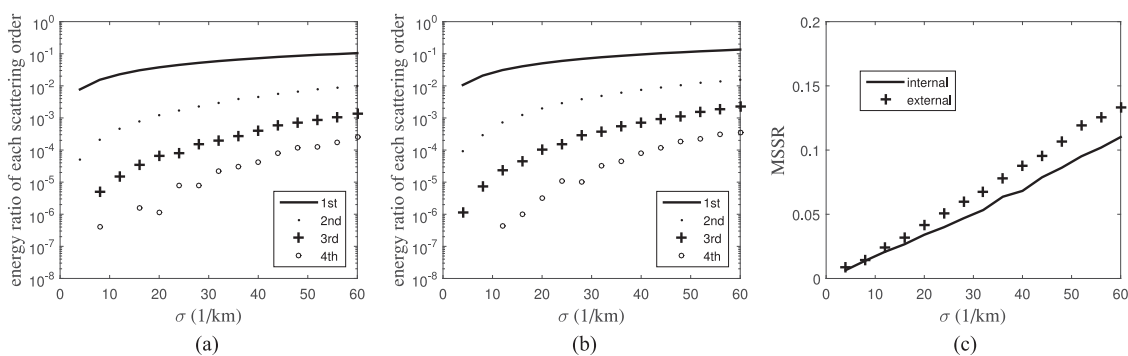
in Fig. 10(a) and (b), for the extinction coefficient $\sigma = 30$, or 60 km^{-1}. For Fig. 10, the data fitting technique has been used.

It is clearly seen in all the figures that the energy ratios of each scattering order and the MSSRs increase with the extinction coefficient for the internal and external mixtures. It can be expected that the multiple scattering effects become stronger for lower visibility weather with larger density of
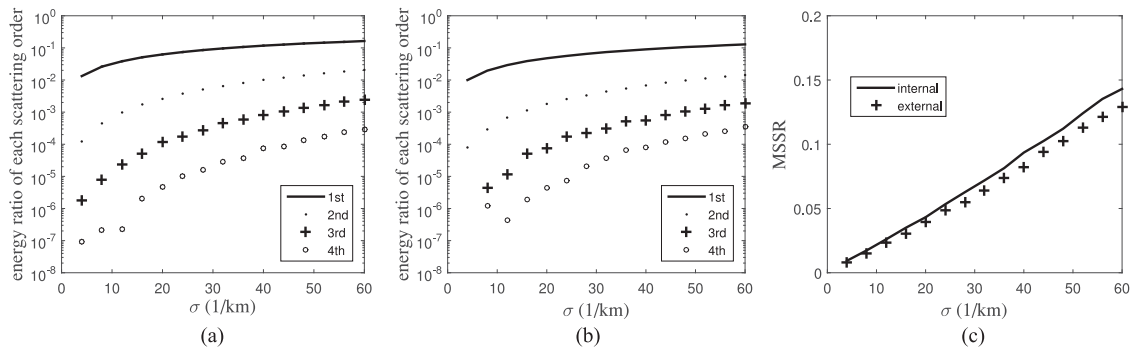
Fig. 8. Scattering properties with respect to the extinction coefficient with the black carbon radius of 5.0 μm. (a) Energy ratio of each scattering order for the internal mixture. (b) Energy ratio of each scattering order for the external mixture. (c) MSSR.

Fig. 9. Scattering properties with respect to the extinction coefficient with the black carbon radius of 5.9 μm. (a) Energy ratio of each scattering order for the internal mixture. (b) Energy ratio of each scattering order for the external mixture. (c) MSSR.
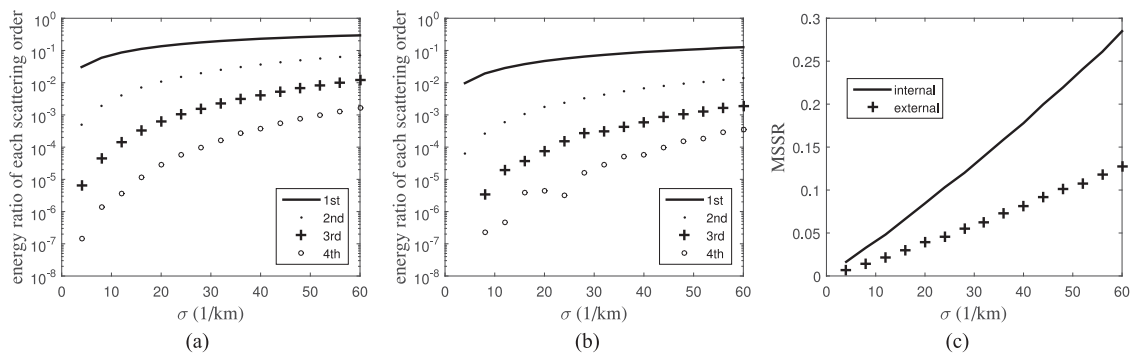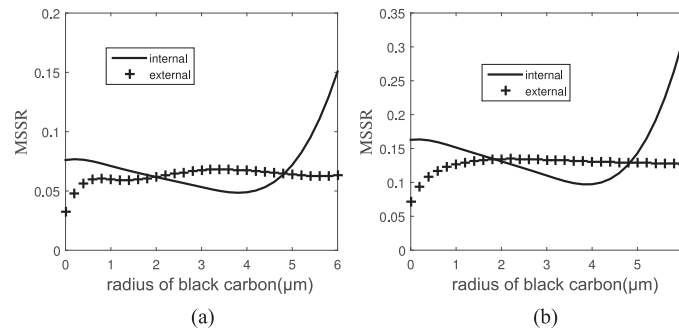

Fig. 10. MSSRs with respect the black carbon radius for internal mixture and external mixture. (a) $\sigma = 30$ km^{-1} (b) $\sigma = 60$ km^{-1}.

aerosols. It is shown in Figs. 5–9(a) and (b) the magnitude differences of the successive scattering orders can be around ten times.

It is seen in Figs. 5–9(a) and c, that for the internal mixture the energy ratios of high scattering orders first decrease slightly and then increase rapidly with the black carbon size. This tendency is clearly illustrated by the solid lines in Fig. 10. As shown in Fig. 10, the inflection point of MSSR for the internal mixture is at around $a = 4$ μm. This can be explained by the single scattering properties of the concentric sphere shown in Table 1. It is seen in Table 1 that for the internal mixture when
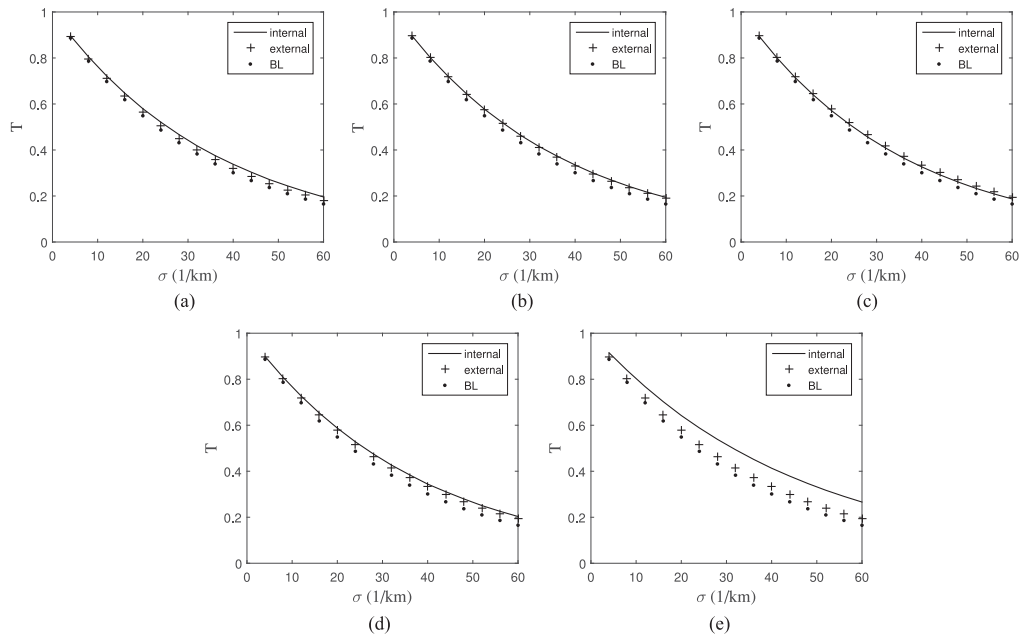
Fig. 11. Transmittances with respect to the extinction coefficient for the internal and external mixtures: the black carbon radii in (a)–(e) are 0.1 μm, 1.0 μm, 3.0 μm, 5.0 μm, 5.9 μm, respectively.

the radius of the black carbon particle is smaller than 3.0 μm, i.e., $a/b < 0.5$, the asymmetry factor keeps almost constant but the single scattering albedo decreases rapidly with a/b., which causes high order scattering components to decrease. For larger size of the black carbon particle, the single scattering albedo decreases, while the asymmetry factor increases rapidly with a/b., and the high order scattering components are seen to be enhanced by the increased asymmetry factor.

Compared to the scattering properties of the internal mixture, the situation of the external mixture is quite different. It is seen in Figs. 5–9(b) and c, that for the external mixture the energy ratios of high scattering orders first increase and then tend to be stable with the black carbon size. This tendency is clearly illustrated by the plus signs in Fig. 10. This can be explained by the single scattering properties of the black carbon particle and the sulfate particle shown in Tables. 2 and 3. It is seen in Table 3, the asymmetry factor and the single scattering albedo of the sulfate particle remain almost constant. However, as seen in Table 2, for $a < 1$ μm, both the asymmetry factor and the single scattering albedo of the black carbon particle increase significantly with the black carbon size. This results in the enhancement of the high order scattering of the external mixture. On the other hand, for $a > 3$ μm, as seen in Table 2, the asymmetry factor and the single scattering albedo of the black carbon particle remain almost constant. Consequently, the MSSR of the external mixture tends to be stable.

In summary the scattering effects and their variations with the black carbon size are significantly different for the internal mixture and the external mixture. The mixing states of the aerosols affect the aerosol multiple scattering effects significantly. It is clearly seen in Figs. 10a and b that the MSSR of the internal mixture is normally larger than that of the external mixture except of the region around $a = 4$ μm, where the MSSR of the internal mixture has the minimum. In particular, as shown in Fig. 9c, the MSSR of internal mixture can as large as twice that of the external mixture for large size of the black carbon particle and low visibility weather.

5. Effects of Aerosol Mixing States on the Light Transmittance

The light transmittances for different black carbon sizes are further calculated using the Monte-Carlo method for the internal and external mixtures, shown in Figs. 11(a)–(e). All the scattering compo-

TABLE 4

Relative Differences of Transmittance for Different Black Carbon Sizes in Percentage

Black carbon radius / μm	0.1	1.0	3.0	5.0	5.9
Internal mixture	18	17	13	23	61
External mixture	9	15	18	17	17

nents are considered in the calculations of the transmittances. In the figures the transmittances calculated using the Beer-Lambert law are also demonstrated as the reference. The Beer-Lambert law is known to give the light transmittance when only the directly transmitted photons contribute to the light received by the detector.

It is seen in the figures that the transmittances of internal and external mixtures calculated by the Monte-Carlo method are always larger than the transmittances calculated using the Beer-Lambert law, as expected. The multiple scattering components may have influences on the light transmittance. It can be seen in the Fig. 11 the transmittance of the internal mixture is normally larger than that of the external mixture, except for the black carbon radius $a = 3$ μm. As shown in Fig. 10(c), for $a = 3$ μm, the transmittance of the internal mixture is slightly smaller than that of the external mixture. This happens when the MSSR of internal mixture becomes smaller than that of external mixture, as shown in Fig. 7(c) and 10.

We further calculated the relative differences of transmittances for internal mixture and external mixture, respectively, for the extinction coefficient of 60 km^{-1}, as shown in Table 4. The reference is the transmittance calculated using the Beer-Lambert law. It can be seen in Table 4 that for the internal mixture the relative difference of transmittance first decreases and then increases with the black carbon size, while for the external mixture the relative difference of transmittance first increases and then almost remains constant. When the black carbon radius $a = 3.0$ μm, the relative difference of transmittance reaches the minimum for the internal mixture as 13%, following the variations of MSSR. In particular, for the internal mixture, the relative difference of transmittance can be as large as 61% for large black carbon size and low visibility weather. In practice when the light transmittance is derived using the Beer-Lambert law, the consequent errors of transmittance induced by the multiple scattering effects can not be ignored. Also they can be significantly different for different mixing states of aerosols.

6. Conclusions

In this paper, based on the single scattering properties of the models of the internal and external mixtures we have for the first time investigated the multiple scattering properties and the light transmittances of the mixed black carbon and sulfate using the Monte-Carlo method. The energy ratios of each scattering order and the MSSRs are demonstrated considering the aerosol extinction coefficient, as well as the black carbon size. The simulation results show that the multiple scattering properties with respect to the black carbon size are quite different for internal and external mixtures. The multiple scattering effects of the internal mixture attenuate first and then strengthen with the black carbon size, while the multiple scattering effects of the external mixture strengthen first and then remain almost invariant. The multiple scattering effects of the internal mixture are normally stronger than those of external mixture, except of the specific range of black carbon size. Both the asymmetry factor and the single scattering albedo are important for determining the multiple scattering effects. Furthermore, it has been found that the consequent errors of light transmittance induced by the multiple scattering effects can be significant and can be quite different for different mixing states of aerosols.

Our simulation results suggest that the aerosol mixing states and the multiple scattering effects be considered in the characterization of the atmospheric aerosols and the evaluation of performances of the optical systems that operate based on the light transmission through the atmosphere. In our

simulations the aerosol systems composing of the black carbon and the sulfate particles are used as the aerosol samples. However, in reality the atmosphere environment can be more complex. The multiple scattering effects of the aerosol systems composing of several aerosol components, mixed with different proportions, different particle size distributions, and different mixing states, are still to be investigated, which can be the possible work in the future.

References

[1] M. Tabrizi, "Influence of multiple scattering of relativistic electrons on the linewidth of Parametric X-ray Radiation produced in the extremely Bragg geometry in the absence of photo absorption," *Radiat. Phys. Chem.*, vol. 127, pp. 7–12, 2016.

[2] R. Buras and B. Mayer, "Efficient unbiased variance reduction techniques for Monte Carlo simulations of radiative transfer in cloudy atmospheres: The solution," *J. Quantitative Spectrosc. Radiative Transfer*, vol. 3, pp. 434–447, 2011.

[3] A. R. Degheidy, M. Sallah, A. Elgarayhi, and S. M. Shaaban, "Optical and radiative-transfer properties of mixed atmospheric aerosols," *Adv. Space Res.*, vol. 55, pp. 1832–1844, 2015.

[4] N. Riemer, M. West, and R. Zaveri, Estimating black carbon aging time scales with a partical_resolved aerosol mode," *Aerosol Sci.*, vol. 41, no. 1, pp. 143–158, 2010.

[5] N. Ma, C. S. Zhao, and T. Muller, "A new method to determine the mixing state of light absobing carbonaceous using the mesured aerosol optical properties and number size distributions," *Atmos. Chem. Phys.*, vol. 12, no. 5, pp. 2381–2397, 2012.

[6] Z. Lan, X. Huang, K. Yu, T. Sun, L. Zeng, and M. Hu, "Light absorption of black carbon aerosol and its enhancement by mixing state in an urban atmosphere in south china," *Atmos. Environ.*, vol. 69, pp. 118–123, 2013.

[7] X. Cui *et al.*, "Radiative absorption enhancement from coatings on black carbon aerosols," *Sci. Total Environ.*, vol. 551, pp. 51–56, 2016.

[8] V. S. Nair, S. S. Babu, K. K. Moorthy, and S. K. Satheesh, "Implications of multiple scattering on the assessment of black carbon aerosol radiative forcing," *J. Quantitative Spectrosc. Radiative Transfer*, vol. 148, pp. 134–140, 2014.

[9] C. Zhou, H. Zhang, and Z. Wang, " Impact of different mixing ways of black carbon and non-absorbing aerosols on the optical properties," *Acta Opt. Sin.*, vol. 33, no. 8, 2013, Art. no. 0829001.

[10] T. Wen, J. Wei, and D. Ma, "Analysis of effect of multiple scattering on laser communication in light haze weather," *Laser Technol.*, vol. 31, no. 5, pp. 500–502, 2007.

[11] H. M. Elkamchouchi and M. A. El-Shimy, "Temporal and spatial impulse response of a water cloud channel for free space optical communication," in *Proc. Nat. Radio Sci. Conf.*, 2008, pp. 1–10.

[12] H. Wang, Y. Zhu, T. Tian, and A. Li, "Characteristics of laser transmission in different types of aerosols," *Acta Phys. Sin.*, vol. 62, no. 2, 2013, Art. no. 024214.

[13] S. Otsuki, "Multiple scattering in turbid media containing chiral components: A MonteCarlo simulation," *Opt. Commun.*, vol. 382, pp. 157–161, 2017.

[14] T. Cheng, Yu Wu, X. Gu, and H. Chen, "Effects of mixing states on the multiple scattering properties of soot aerosols," *Opt. Exp.*, vol. 23, no. 8, pp. 10808–10821, 2015.

[15] H. Wang and X. Sun, "Multiple scattering of light by water cloud droplets with external and internal mixing of black carbon aerosols," *Chin. Phys. B*, vol. 21, no. 5, 2012, Art. no. 054204.

[16] H. Zhang, C. Zhou, Z. Wang, S. Zhao, and J. Li, "The influence of different black carbon and sulfate mixing methods on their optical and radiative properties," *J. Quantitative Spectrosc. Radiative Transfer*, vol. 161, pp. 105–116, 2015.

[17] J. C. Maxwell Garnett, "XII. Colours in metal glasses and in metallic films," *Trans. Roy. Soc. Lond. A*, vol. 203, pp. 385–420, 1904.

[18] S. A. Prahl, M. Keijzer, S. J. Jacques, and A. J. Welch, "A Monte Carlo model of light propagation in tissue," *Proc. SPIE*, vol. 5, pp. 102–111, 1989.

[19] A. N. Witt "Multiple scattering in reflection nebulae. I. A Monte Carlo approach," *Astrophys. J. Suppl. Ser.*, vol. 35, pp. 1–6, 1977.

[20] Y. Ma, W. Liu, Y. Cui, and X. Xiong, "Multiple-scattering effects of atmosphere aerosols on light-transmission measurements," *Opt. Rev.*, vol. 24, no. 4, pp. 590–599, 2017.

[21] P. R. J. North, J. A. B. Rosette, and J. C. Suárez, "A monte carlo radiative transfer model of satellite waveform LiDAR," *Int. J. Remote Sens.*, vol. 5, pp. 1343–1358, 2010.

[22] Z. Xu and P. Wang, "A modified multiple scattering model based on Monte Carlo method," *J. Naval Univ. Eng.*, vol. 22, no. 1, pp. 50–61, 2010.

[23] X. Sun, S. Xiao, L. Wan, H. Wang, and S. Jin, "Monte Carlo simulation of polarization lidar multiple scattering depolarization by water cloud," *Chin. J. Lasers*, vol. 42, no. 11, 2015, Art. no. 1113005.